Planetary Probe Entry Atmosphere Estimation Using Synthetic Air Data System

Christopher D. Karlgaard*
Analytical Mechanics Associates, Inc., Hampton, VA

Mark Schoenenberger†
NASA Langley Research Center, Hampton, VA

This paper develops an atmospheric state estimator based on inertial acceleration and angular rate measurements combined with an assumed vehicle aerodynamic model. The approach utilizes the full navigation state of the vehicle (position, velocity, and attitude) to recast the vehicle aerodynamic model to be a function solely of the atmospheric state (density, pressure, and winds). Force and moment measurements are based on vehicle sensed accelerations and angular rates. These measurements are combined with an aerodynamic model and a Kalman-Schmidt filter to estimate the atmospheric conditions. The new method is applied to data from the Mars Science Laboratory mission, which landed the Curiosity rover on the surface of Mars in August 2012. The results of the new estimation algorithm are compared with results from a Flush Air Data Sensing algorithm based on onboard pressure measurements on the vehicle forebody. The comparison indicates that the new proposed estimation method provides estimates consistent with the air data measurements, without the use of pressure measurements. Implications for future missions such as the Mars 2020 entry capsule are described.

Nomenclature

$\boldsymbol{C}$	=	state-parameter covariance
$\boldsymbol{\mathcal{F}}$	=	aerodynamic force, N
$\boldsymbol{F}$	=	linearization of $\boldsymbol{f}$ with respect to $\boldsymbol{x}$
$\boldsymbol{f}$	=	process model
$\boldsymbol{G}$	=	linearization of $\boldsymbol{f}$ with respect to $\boldsymbol{u}$
g	=	gravitational acceleration, m/s^2
$\boldsymbol{H}$	=	linearization of $\boldsymbol{h}$ with respect to $\boldsymbol{x}$
$\boldsymbol{h}$	=	measurement model
$\boldsymbol{I}$	=	identity matrix
$\boldsymbol{\mathcal{I}}$	=	vehicle inertia, kg-m^2
$\boldsymbol{J}$	=	linearization of $\boldsymbol{h}$ with respect to $\boldsymbol{u}$
$\boldsymbol{K}$	=	filter gain
k	=	integer time index
$\boldsymbol{\mathcal{M}}$	=	aerodynamic moment, N-m
M	=	Mach number
$\boldsymbol{P}$	=	covariance of $\boldsymbol{x}$
p_s	=	static pressure, Pa
$\boldsymbol{Q}$	=	process noise spectral density

*Supervising Engineer, Senior Member AIAA.
†Aerospace Engineer, Atmospheric Flight and Entry Systems Branch, Senior Member AIAA.

$\tilde{\boldsymbol{Q}}$	=	process noise covariance
$\boldsymbol{R}$	=	measurement error covariance matrix
$\Re$	=	specific gas constant, J/kg-K
r	=	radius, m
T	=	atmospheric temperature, K
v_n, v_e, v_d	=	vehicle planet-relative north, east, and down velocity components, m/s
w_n, w_e, w_d	=	north, east, and down wind velocity components, m/s
$\boldsymbol{x}$	=	atmospheric state vector
Θ	=	longitude, rad
θ, ϕ, ψ	=	vehicle pitch, roll, and yaw attitude angles, rad
Λ	=	declination, rad
$\boldsymbol{\lambda}$	=	aerodatabase uncertainty factors
μ	=	gravitational parameter, m^3/s^2
$\boldsymbol{\nu}$	=	vehicle inertial state
ρ	=	density, kg/m^3
$\boldsymbol{\Phi}$	=	state transition matrix

I. Introduction

NASA has developed an Entry, Descent, and Landing (EDL) technology development roadmap[1] to guide investment strategies for increased EDL capabilities and robustness. One area of emphasis is on the development of precision landing capabilities achieved through improved environment/atmosphere characterization and EDL instrumentation for validation of engineering models and ground testing procedures. One approach that can be used to address these areas is the implementation of a Flush Air Data Sensing (FADS) system, which utilizes an array of pressure ports installed in the vehicle forebody to measure the pressure distribution during entry. These pressure measurements can be processed to estimate the freestream aerodynamic state (such as flow angles, Mach number, and dynamic pressure), atmospheric conditions (density, pressure, and winds) and vehicle aerodynamics. These sensors can be used for post-flight trajectory reconstruction and model validation, but also have the potential to be used to augment the on-board flight control system by providing estimates of density and winds if the data processing algorithms can be implemented in real-time.

Incorporation of pressure measurements into the heatshield of an entry vehicle is not trivial. Implementation of a reliable FADS system typically involves hardware development and qualification, optimization of pressure port layout, sensor calibration, ground testing to ensure pressure port and thermal protection system integrity, etc., which can be costly. Additionally, a FADS system is subject to risks of sensor failures and other hardware anomalies.

Typically, planetary entry atmosphere reconstruction is performed using vehicle aerodynamic models when FADS instrumentation is not available. The concept of utilizing vehicle aerodynamic models for entry probe atmosphere estimation is not new. In fact, the concept goes back to a 1963 NASA report[4] in which a proposal was made to "invert" the entry physics problem by solving for atmospheric density, given acceleration measurements and a model of vehicle drag. The concept was further developed to estimate aerodynamic flow angles in later papers, such as Ref. 5. The methodology was validated using entry vehicle test flights on Earth, with known atmospheric conditions,[6] and was subsequently applied to the reconstruction of the atmosphere of Mars based on measurements from the Viking entry probes.[7] Since Viking, the approach has been utilized on virtually every planetary atmospheric entry reconstruction to date. A recent thesis[8] documents the development and history of the algorithm, from its inception in the early 1960s to the most recent application of the method for the Mars Science Laboratory mission.[9]

The previous approaches make use of measured accelerations and known aerodynamic models to solve for the freestream conditions by first computing density from the axial force coefficient and axial acceleration. The reconstructed density is then used to integrate the hydrostatic equation to estimate static pressure. The ratio of normal to axial and side to axial forces are then utilized to estimate the angles of attack and sideslip, respectively. The process can be iterated at each instant in time to improve the estimates; for instance, a combined inner and outer loop is implemented in Ref. 9 for solving the aerodynamic flow angles (inner loop) and freestream atmospheric conditions (outer loop). Note that the algorithm is completely deterministic in nature, although uncertainties in the reconstructed quantities can be computed using linear covariance analysis techniques.[8,9] Estimation of winds from aerodynamics has not been addressed directly; some approaches instead rely on a post-processing method such as that proposed in Ref. 10 for computing winds from flow angles and the navigation state.

A recently proposed alternative to a traditional FADS system is a technique known as a Synthetic Air Data Sensing (SADS) system. The SADS approach makes use of an aerodynamic model of the vehicle, combined with acceleration and angular rate measurements on an onboard Inertial Measurement Unit (IMU) to estimate the freestream aerodynamic and atmospheric conditions. A SADS system can be used either as a backup, or as a low-cost alternative to a traditional FADS system.

This paper extends the SADS concept to the planetary probe entry vehicle atmosphere estimation problem. The method developed in this paper is most similar to that of Refs. 12 and 13, in which a model of the vehicle dynamics is combined with an inertial navigation system to produce estimates of the atmospheric winds using a Kalman filter method for improved navigation and flight control. One important drawback of these approaches is that the atmospheric density and pressure are not estimated in the filter; instead these are assumed to be known as a function of altitude. This assumption is not suitable for planetary probe entry estimation in which the atmospheric properties are highly uncertain. In this paper, the concept of atmospheric estimation aided by a vehicle aerodynamics model is extended to estimate freestream density and pressure in addition to winds. This new approach is developed for planetary entry state estimation, but it is anticipated that the method can be applied to other applications such as high speed aircraft.

II. Atmospheric State Estimation

The new approach for SADS-based state estimation proposed in this paper makes use of the full state from the on-board navigation system (position, velocity, and attitude) combined with the vehicle aerodynamic database to directly estimate the atmospheric conditions. The estimation algorithm is aided by both high-fidelity atmospheric models tabulated vs. altitude and simplified atmospheric models that are propagated along the trajectory within the algorithm.

A. Measurement Model

This work assumes that an aerodynamic model of the entry capsule is available, in which force and moment coefficients can be calculated from a given flight condition (angle of attack, sideslip, Mach number, etc.). It is assumed the aerodynamic model produces outputs in some known coordinate frame, such as that shown in Figure 1. Dimensional aerodynamic forces and moments acting on the vehicle are then computed using the relations

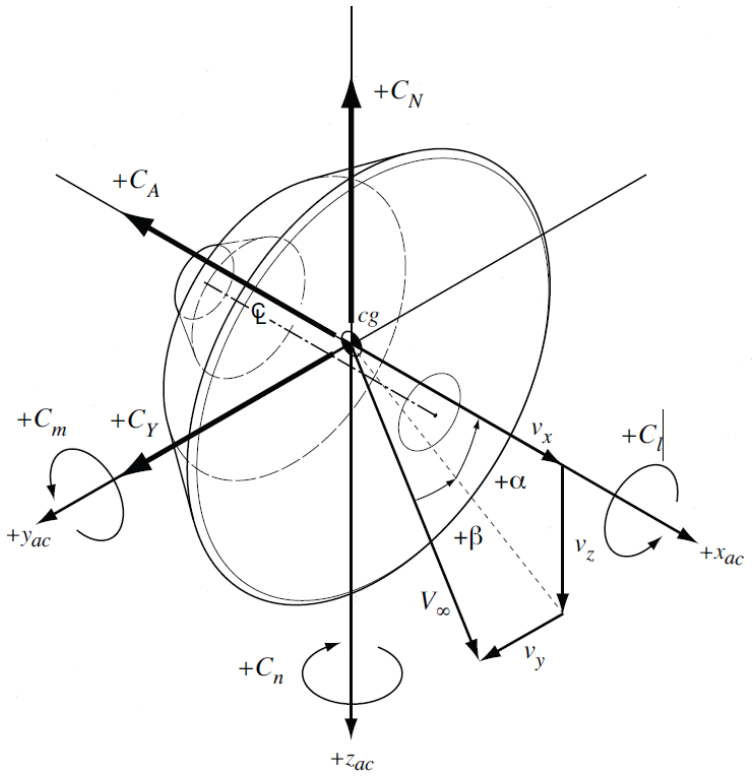

Figure 1: Body Coordinate System

$$\boldsymbol{\mathcal{F}} = m\boldsymbol{a} = \frac{1}{2}\rho V^2 S \left\{ \begin{array}{c} -C_A\left(\alpha,\beta,M,\boldsymbol{\lambda}\right) \\ C_Y\left(\alpha,\beta,M,\boldsymbol{\lambda}\right) \\ -C_Z\left(\alpha,\beta,M,\boldsymbol{\lambda}\right) \end{array} \right\} \tag{1}$$

$$\boldsymbol{\mathcal{M}} = \mathcal{I}\dot{\boldsymbol{\omega}} + \boldsymbol{\omega} \times \mathcal{I}\boldsymbol{\omega} = \frac{1}{2}\rho V^2 S b \left\{ \begin{array}{c} C_l\left(\alpha,\beta,M,\boldsymbol{\lambda}\right) \\ C_m\left(\alpha,\beta,M,\boldsymbol{\lambda}\right) \\ C_n\left(\alpha,\beta,M,\boldsymbol{\lambda}\right) \end{array} \right\} \tag{2}$$

where $\boldsymbol{\lambda}$ is a vector comprised of the aerodatabase uncertainty factors, which are a collection of adders and multipliers used to perturb the aerodynamics.

Given that dynamic pressure is a function of vehicle velocity, winds, and density; Mach number is a function of velocity, winds, density, and pressure; aerodynamic flow angles are functions of velocity, winds, and attitude, the aerodynamic force and moment model can be recast into the form

$$m\boldsymbol{a} = \boldsymbol{\mathcal{F}}\left(\boldsymbol{x},\boldsymbol{u}\right) \tag{3}$$

$$\mathcal{I}\dot{\boldsymbol{\omega}} + \boldsymbol{\omega} \times \mathcal{I}\boldsymbol{\omega} = \boldsymbol{\mathcal{M}}\left(\boldsymbol{x},\boldsymbol{u}\right) \tag{4}$$

where $\boldsymbol{x} = [\rho, p_s, w_n, w_e, w_d]^\intercal$ is the atmospheric state, $\boldsymbol{u} = [\boldsymbol{\nu}, \boldsymbol{\lambda}]^\intercal$ are model parameters, and the vehicle planet-relative navigation state is $\boldsymbol{\nu} = [r, \Theta, \Lambda, v_n, v_e, v_d, \phi, \theta, \psi]^\intercal$.

High-fidelity atmosphere models can also be incorporated into the state estimate as prior information. These atmosphere models are assumed to be computationally intensive such that implementation within the algorithm is infeasible. Instead, the high-fidelity atmosphere model data can be incorporated using table look-ups where the atmospheric conditions and uncertainties are tabulated as a function of altitude along some nominal trajectory. The model of this form produces an estimate of the atmospheric conditions, along with an associated error covariance matrix.

The aerodynamic force and moment and high-fidelity atmosphere models can be combined into a single expression, $\boldsymbol{z} = \boldsymbol{h}\left(\boldsymbol{x},\boldsymbol{u}\right)$, where $\boldsymbol{h} = \left[\boldsymbol{\mathcal{F}}\left(\boldsymbol{x},\boldsymbol{u}\right), \boldsymbol{\mathcal{M}}\left(\boldsymbol{x},\boldsymbol{u}\right), \boldsymbol{x}\right]^\intercal$. Note that the measurement error covariance matrix $\boldsymbol{R}$ is a function of both sensor and mass property uncertainties.

B. Process Model

A low-fidelity model of the change in atmospheric conditions along the trajectory can be derived from basic idealized relations such as the hydrostatic equation and the perfect gas law. Such simplified relationships are suitable for implementation in the algorithm for propagating the atmospheric state estimate forward between aerodynamic measurements, which are assumed to occur at a reasonably high rate (several samples per second) along the trajectory. Since the simplified model involves idealized approximations, uncertainties in the model can be accounted for with process noise.

A model for the rate of change in static pressure can be found by rewriting the hydrostatic equation as the time derivative of pressure along a given trajectory, namely

$$\dot{p}_s = \rho g v_d \tag{5}$$

Similarly, a model for the rate of change in density along the trajectory can be derived from the perfect gas law, with the assumption that the atmosphere is locally isothermal ($\dot{T} \approx 0$) between measurement samples. The equation is of the form

$$\dot{\rho} = \frac{\dot{p}_s}{\Re T} = \frac{\dot{p}_s \rho}{p_s} = \frac{g v_d \rho^2}{p_s} \tag{6}$$

A reasonable simplified model for the rate of change in atmospheric winds is to assume a random walk model where the deterministic portion of the model is simply $\dot{w}_n = \dot{w}_e = \dot{w}_d = 0$. Thus, the low fidelity model can be written in the form

$$\dot{\boldsymbol{x}} = \boldsymbol{f}\left(\boldsymbol{x},\boldsymbol{u}\right) + \boldsymbol{\eta} \tag{7}$$

where $\boldsymbol{\eta}$ is a process uncertainty term that is assumed to be zero mean with spectral density $\boldsymbol{Q}$, and

$$\boldsymbol{f}\left(\boldsymbol{x},\boldsymbol{u}\right) = \left\{ \begin{array}{c} g v_d \rho^2 / p_s \\ \rho g v_d \\ 0 \\ 0 \\ 0 \end{array} \right\} \tag{8}$$

The continuous model in Eq. (7) can be transformed to a discrete model of the form,

$$\boldsymbol{x}_{k+1} = \boldsymbol{x}_k + \boldsymbol{f}\left(\boldsymbol{x}_k, \boldsymbol{u}_k\right)\Delta t \tag{9}$$

which is suitable for propagation between measurements.

C. Data Fusion Algorithm

The atmospheric state estimate can be determined from a fusion of the available data sources, including the aerodynamic force and moment measurements, and information from the low and high fidelity models. The proposed algorithm is in the form of an Iterated Extended Kalman-Schmidt Filter (IEKSF)[15] incorporating the process and measurement models described above. The IEKSF approach incorporates parameter uncertainties in the process and measurement models, thus producing a realistic state covariance estimate.

The algorithm is structured as a predictor-corrector method, in which state estimates are propagated between measurement samples using the relations

$$\bar{\boldsymbol{x}}_{k+1} = \hat{\boldsymbol{x}}_k + \boldsymbol{f}\left(\bar{\boldsymbol{x}}_k, \bar{\boldsymbol{u}}_k\right)\Delta t \tag{10}$$

$$\bar{\boldsymbol{P}}_{k+1} = \boldsymbol{\Phi}_k\hat{\boldsymbol{P}}_k\boldsymbol{\Phi}_k^\intercal + \boldsymbol{\Phi}_k\hat{\boldsymbol{C}}_k\boldsymbol{G}_k^\intercal + \boldsymbol{G}_k\boldsymbol{C}_k^\intercal\boldsymbol{\Phi}_k^\intercal + \boldsymbol{G}_k\boldsymbol{\Omega}_k\boldsymbol{G}_k^\intercal + \tilde{\boldsymbol{Q}}_k \tag{11}$$

$$\bar{\boldsymbol{C}}_{k+1} = \boldsymbol{\Phi}_k\hat{\boldsymbol{C}}_k + \boldsymbol{G}_k\boldsymbol{\Omega}_k \tag{12}$$

where $\boldsymbol{\Phi}_k$ is the state transition matrix and $\tilde{\boldsymbol{Q}}_k$ is the discrete-time process noise covariance. These quantities can be jointly calculated from the Van Loan matrix integral,[16] given by

$$\exp\left(\begin{bmatrix} -\boldsymbol{F}_k & \boldsymbol{Q}_k \\ \boldsymbol{0} & \boldsymbol{F}_k \end{bmatrix}\Delta t\right) = \begin{bmatrix} \boldsymbol{X}_{11} & \boldsymbol{X}_{12} \\ \boldsymbol{0} & \boldsymbol{X}_{22} \end{bmatrix} = \begin{bmatrix} \boldsymbol{X}_{11} & \boldsymbol{\Phi}_k^{-1}\tilde{\boldsymbol{Q}}_k \\ \boldsymbol{0} & \boldsymbol{\Phi}_k^\intercal \end{bmatrix} \tag{13}$$

which leads to the result $\boldsymbol{\Phi}_k = \boldsymbol{X}_{22}^\intercal$ and $\tilde{\boldsymbol{Q}}_k = \boldsymbol{\Phi}_k\boldsymbol{X}_{12}$. Assuming a reasonably fast integration step, these quantities can be approximated by $\boldsymbol{\Phi}_k \approx \boldsymbol{I} + \boldsymbol{F}_k\Delta t$ and $\tilde{\boldsymbol{Q}}_k \approx \boldsymbol{Q}_k\Delta t$.

The measurement update is an iterative process to solve a nonlinear least squares regression problem, involving the measurement and the state prediction as observations. The process is given by the equations

$$\boldsymbol{S}_{k,i} = \boldsymbol{H}_{k,i}\bar{\boldsymbol{P}}_{k,i}\boldsymbol{H}_{k,i}^\intercal + \boldsymbol{H}_{k,i}\bar{\boldsymbol{C}}_k\boldsymbol{L}_k^\intercal + \boldsymbol{L}_k\bar{\boldsymbol{C}}_k^\intercal\boldsymbol{H}_{k,i}^\intercal + \boldsymbol{R}_k \tag{14}$$

$$\boldsymbol{K}_{k,i} = \left[\bar{\boldsymbol{P}}_k\boldsymbol{H}_{k,i}^\intercal + \bar{\boldsymbol{C}}_k\boldsymbol{L}_k^\intercal\right]\boldsymbol{S}_{k,i}^{-1} \tag{15}$$

$$\hat{\boldsymbol{x}}_{k,i+1} = \bar{\boldsymbol{x}}_k + \boldsymbol{K}_{k,i}\left[\boldsymbol{z}_k - \boldsymbol{h}\left(\hat{\boldsymbol{x}}_{k,i}, \boldsymbol{u}_k\right) - \boldsymbol{H}_{k,i}\left(\bar{\boldsymbol{x}}_k - \hat{\boldsymbol{x}}_{k,i}\right)\right] \tag{16}$$

Equations (14)–(16) are iterated until convergence or until reaching a prescribed iteration limit. After the iteration is complete, the state covariance and state-parameter covariance matrices can be computed as

$$\hat{\boldsymbol{P}}_k = \bar{\boldsymbol{P}}_k - \boldsymbol{K}_k\boldsymbol{S}_k\boldsymbol{K}_k^\intercal \tag{17}$$

$$\hat{\boldsymbol{C}}_k = \bar{\boldsymbol{C}}_k - \boldsymbol{K}_k\left[\boldsymbol{H}_k\bar{\boldsymbol{C}}_k + \boldsymbol{L}_k\boldsymbol{\Omega}_k\right] \tag{18}$$

The Kalman-Schmidt filter approach has the advantage of providing optimal state estimates that account for systematic parameter uncertainties to produce a realistic state covariance estimate.

D. Aerodynamic State Transformations

The atmospheric state (winds, pressure, and density) are outputs of the proposed SADS data processing algorithm. The atmospheric state can readily be combined with the INS state solution to produce estimates of aerodynamic states, including angle of attack, sideslip, Mach number, and dynamic pressure. Uncertainties can be mapped from the atmospheric and INS states into the aerodynamic states through linear covariance analysis. The equations of the transformation from atmospheric and INS states to aerodynamic states are readily available in various sources such as Ref. 18 and are not repeated here.

III. Application to Mars Science Laboratory

On August 5th 2012, the Mars Science Laboratory (MSL) entry vehicle successfully entered the atmosphere of Mars and landed the Curiosity rover safely on the surface of the planet in Gale crater. The MSL entry vehicle

was comprised of a 70-degree sphere-cone heatshield and backshell consisting of a stack of three truncated cones. The forebody was similar to the heatshield geometry developed for the Viking Mars landers. Phenolic Impregnated Carbon Ablator (PICA) was used for the thermal protection system material. The backshell configuration was also similar to Viking, with a third cone section added to accommodate the parachute volume. The MSL vehicle as-built outer mold line is shown in Fig. 2(a).[19] During most of entry, the capsule used a radial center of mass offset to fly at an angle of attack (approximately 16 degrees at hypersonic conditions). This attitude produced lift to fly a guided entry profile, reducing the landing footprint to a much smaller size than any previous Mars mission. To fly the guided entry, the vehicle carried four pairs of Reaction Control System (RCS) jets to perform maneuvers and damp rates. The four pairs of jets could be fired rapidly in different combinations to provide control torque about any axis by modulating the pulses of the jet.

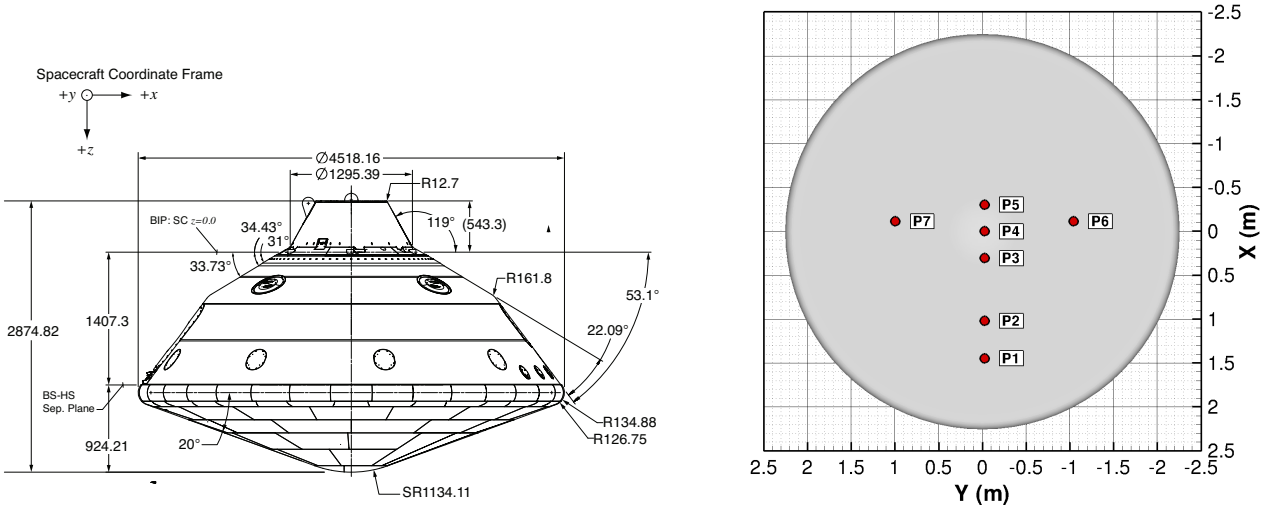

(a) As Built MSL Outer Mold Line

(b) MEDLI/MEADS Geometry (Looking Aft)

Figure 2: Vehicle Geometry

MSL carried with it an instrumentation package designed to measure the aerodynamic and aerothermal environments during atmospheric entry. This instrumentation package was known as the MSL Entry, Descent, and Landing Instrumentation (MEDLI),[20] which consisted of three major subsystems: the Mars Entry Atmospheric Data System (MEADS), the MEDLI Integrated Sensor Plugs (MISP), and the Sensor Support Electronics (SSE). The MEADS consisted of seven pressure transducers connected to flush orifices in the heat shield to measure pressures across the vehicle forebody. The MISP devices were a system of seven thermocouple and recession sensors that provided aerothermal measurements of the heat shield performance. The SSE provided power to the sensors, conditioned their signals, and transmitted the data to storage on the Curiosity rover. The MEDLI sensors provided measurements that were used for trajectory reconstruction and engineering validation of aerodynamic, atmospheric, and thermal protection system models in addition to Earth-based systems testing procedures. The MEDLI data and its usage for reconstructing the aerodynamic and aerothermal performance of the MSL entry vehicle are described in Refs. 21–29.

The aerodynamic forces and moments were sensed by the on-board IMU in the form of acceleration and angular rate measurements at a frequency of 200 Hz. The dimensional aerodynamic forces and moments were calculated from these measurements, combined with mass and inertia models of the vehicle. Forces and moments due to the RCS firing were subtracted from the total force and moment measurements. The results were found to be sensitive to vibration and noise associated with RCS firings, so a low-pass optimal Fourier filter with a cut-off frequency of 2 Hz was applied to smooth the data.[26] The raw and filtered aerodynamics are shown in Figure 3. Note the increase in noise around the time of bank reversals, which correlate with the times of RCS thruster commands shown in Figure 4. The filtered side/normal and pitch/yaw moments are shown in Figure 5.

The SADS estimator was initialized at 580 s in the MSL EDL timeline, corresponding to an altitude of approximately 66.15 km. The initial atmospheric state was based on pre-flight mesoscale models.[32] The air data filter was implemented to run at a rate of 64 Hz to match the rate of the on-board navigation state. The filter was terminated at a time of 800 s, at an altitude of 7.10 km. Given the sensitivity of moments to the RCS noise, the filter was set to ignore moment measurements while the RCS was active and rely solely on force measurements. The estimator made use of the post-flight reconstructed aerodynamic model described in Ref. 26.

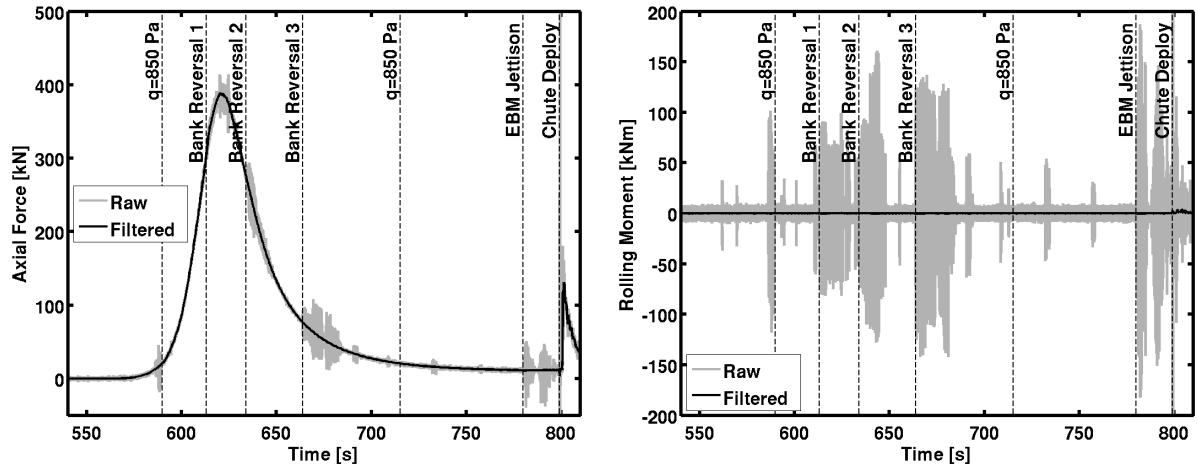

(a) Axial Force

(b) Rolling Moment

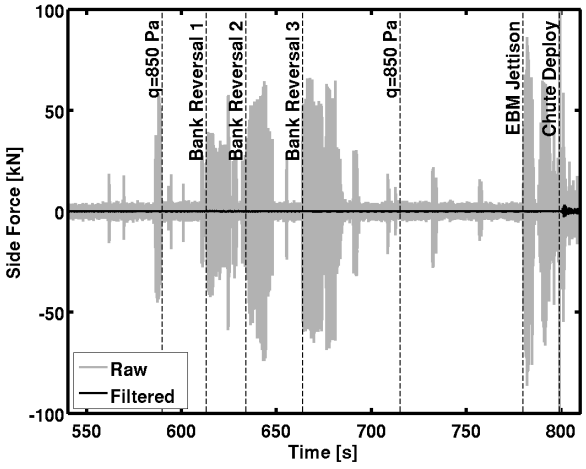

(c) Side Force

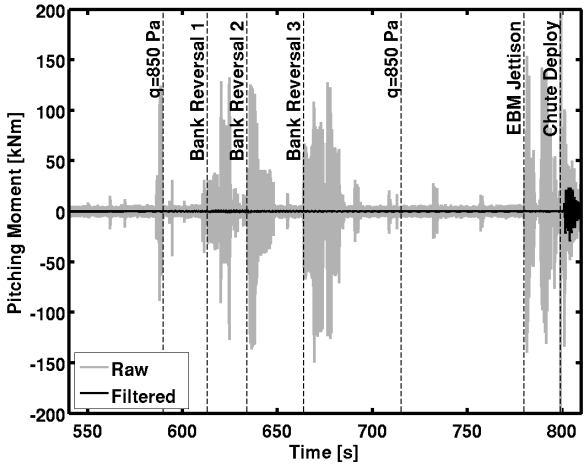

(d) Pitching Moment

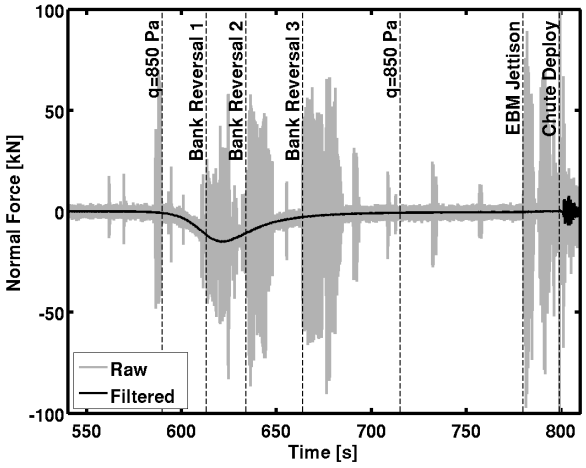

(e) Normal Force

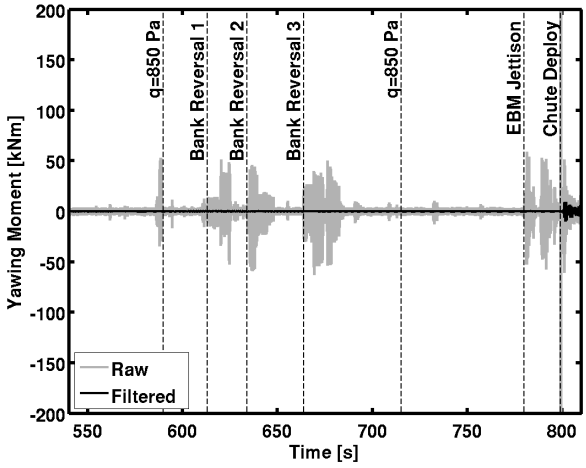

(f) Yawing Moment

Figure 3: Measured Aerodynamic Forces and Moments

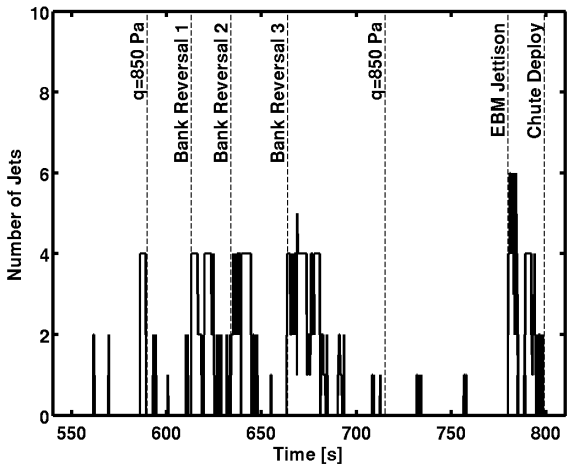

Figure 4: RCS Firing

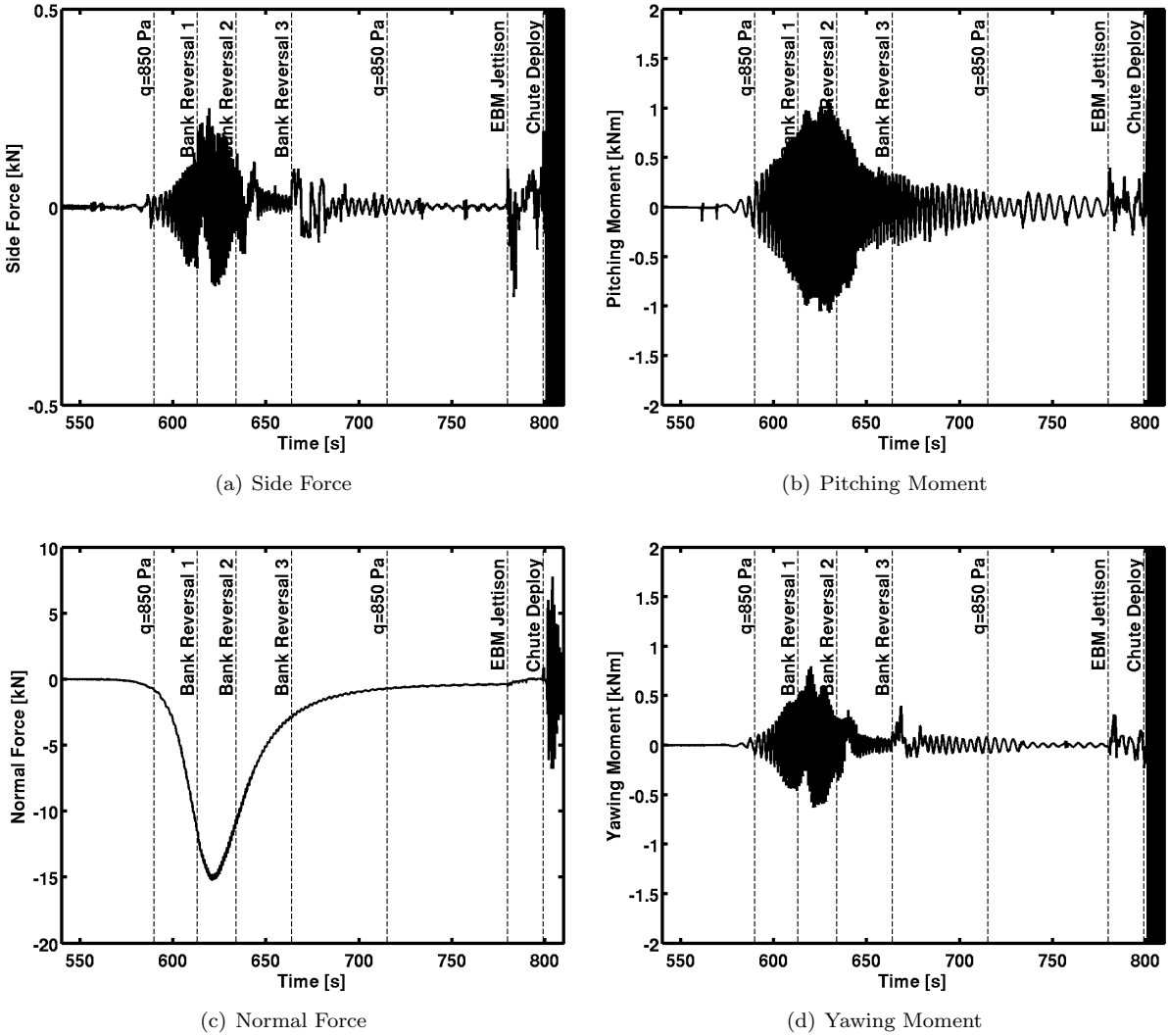

(a) Side Force

(b) Pitching Moment

(c) Normal Force

(d) Yawing Moment

Figure 5: Filtered Aerodynamic Forces and Moments

Results of the SADS estimator are shown in the following figures. The results are compared to true air data estimation results from the MEADS pressure measurement data, described in Reference 29. In the following figures, the pressure transducer-based estimation is labeled FADS, and the new synthetic air data solution developed in this paper is labeled as SADS.

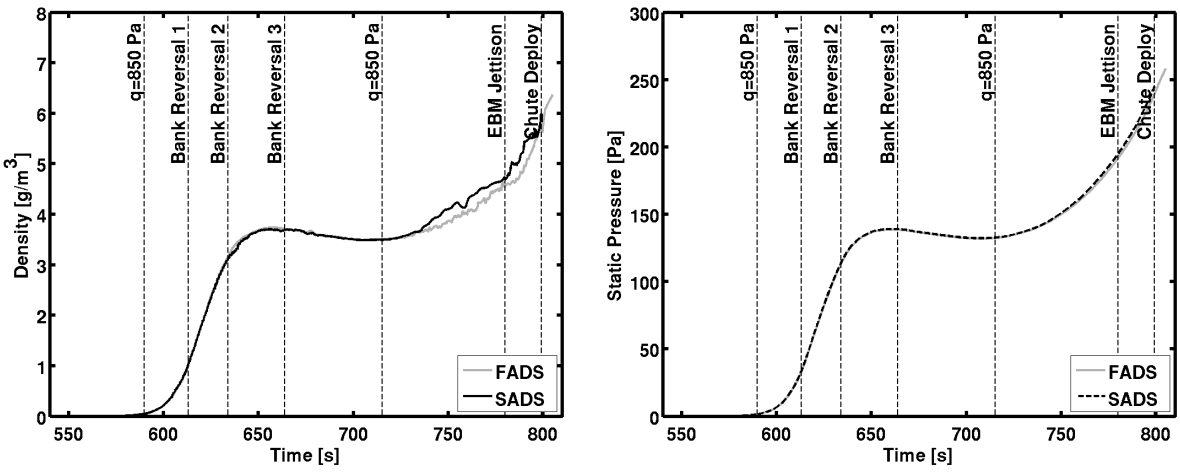

(a) Density

(b) Pressure

Figure 6: Atmosphere

The atmospheric density and pressure estimates are shown in Figure 6. The two solutions give consistent results. Some differences are apparent in the low supersonic flight regime, below 850 Pa dynamic pressure. These differences are consistent with those between the post-flight reconstructed axial force coefficient and the reconciled aerodynamics, as described in Ref. 26. These differences are most likely attributable to transducer instrumentation errors in low pressure ranges that are outside their design requirements. Differences in density and pressure estimates are within 0.5% over the range in which the transducers were calibrated (above 850 Pa dynamic pressure).

The estimated winds along the trajectory are shown in Figure 7. The two methods produce consistent estimates, although the SADS exhibits more noise in the estimate. The noise is likely a combination of higher data rate (64 Hz compared to the 8 Hz FADS solution) and errors due to vibrations in the accelerometer. The mean profile and general trends follow the FADS solution. This result is important as it indicates the ability of the SADS approach to mimic a true FADS without the use of pressure sensors. The reconstructed winds from these two methods are consistent with observed vehicle dynamics and guidance response.[34,35]

The dynamic pressure and Mach estimates of are shown in Figure 8. The methods are in agreement over the entry trajectory. Differences in the dynamic pressure and Mach estimates are on the order of 0.5% and 0.05, respectively, in region where the pressure measurements were calibrated. The aerodynamic flow angle estimates are shown in Figure 9. The FADS and SADS solutions are in agreement, with differences on the order of 0.25 deg, thus indicating the SADS method is able to provide an estimate of the vehicle state that is consistent with a true air data system.

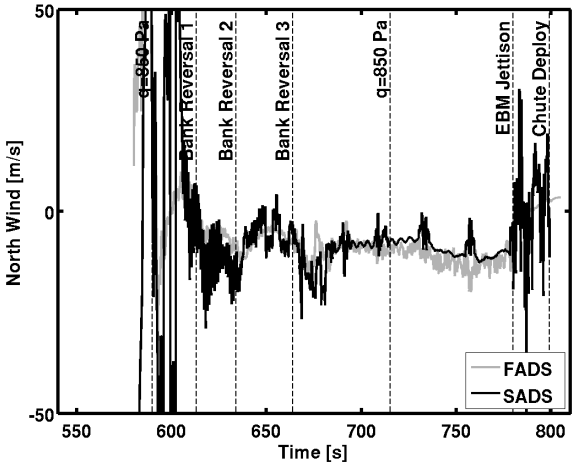

(a) North Wind

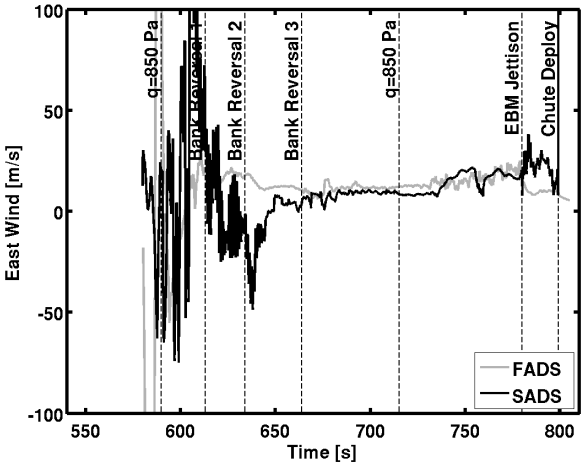

(b) East Wind

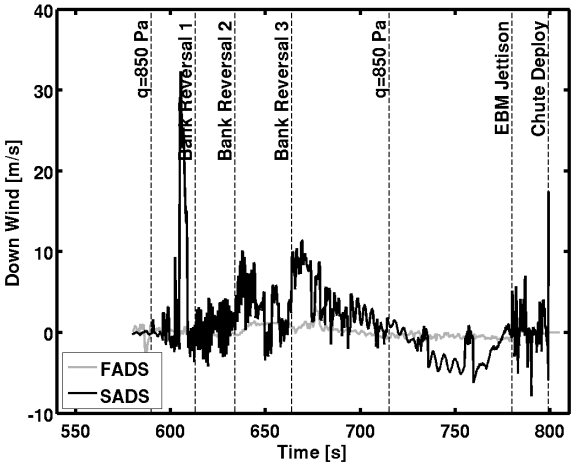

(c) Down Wind

Figure 7: Winds

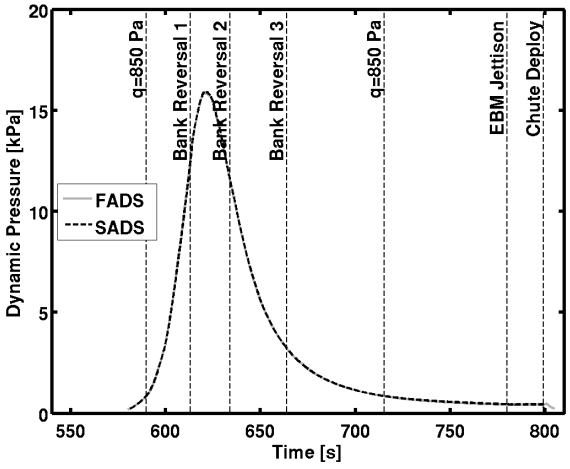

(a) Dynamic Pressure

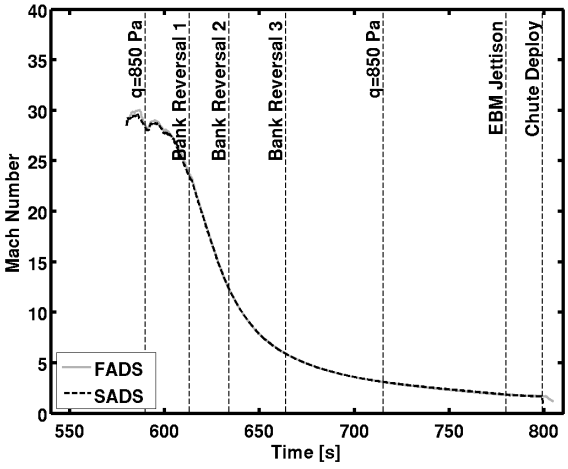

(b) Mach Number

Figure 8: Dynamic Pressure and Mach Number

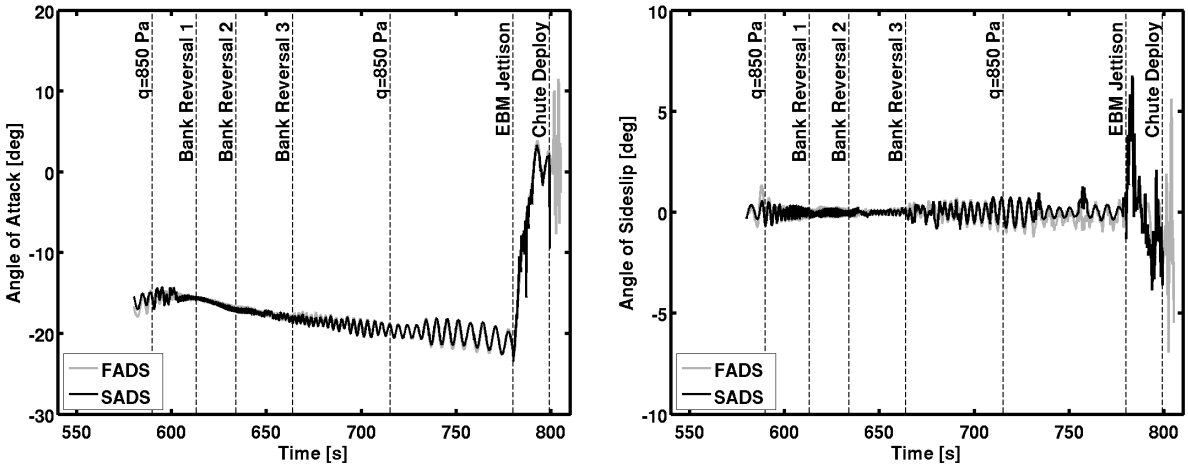

(a) Angle of Attack

(b) Angle of Sideslip

Figure 9: Aerodynamic Angles

IV. Application to the Mars 2020 Mission

Another MEDLI-like system of instruments is planned to be flown on the Mars 2020 mission. This instrumentation system, known as MEDLI2,[38] will acquire FADS pressure data to be used for the reconstruction of atmospheric states and vehicle aerodynamics during entry. The focus of the pressure system on MEDLI2 is geared toward estimating aerodynamics in the supersonic regime of flight, where some questions remain regarding the aerodynamic reconstruction of MSL.[26] To this end, the forebody pressure system will carry one transducer with a full scale range of 35 kPa (the same as MSL transducers) to measure stagnation pressure over the entire entry trajectory (which in turn yields estimates of dynamic pressure and density), and six transducers with a full scale range of 7 kPa to more accurately measure the atmosphere and aerodynamics in the supersonic regime of flight (roughly Mach 6 and below). In addition, one transducer will be installed on the backshell to measure the base pressure and its contribution to drag. The forebody pressure port layout corresponding to the current MEDLI2 design is shown in Fig. 10. Note that port P1 corresponds to the hypersonic pressure transducer.

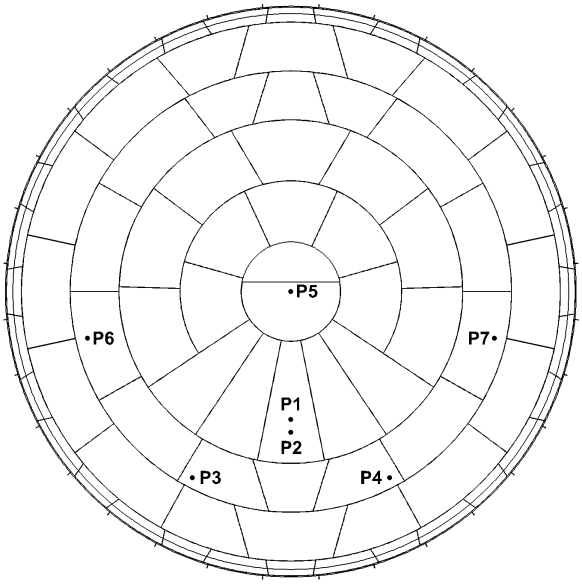

Figure 10: Mars 2020 Pressure Port Arrangement

Since the focus of this instrumentation is on supersonic measurements, only one hypersonic transducer is available

to provide estimates of the atmospheric conditions during entry for a large altitude range before the supersonic transducers de-saturate at 7 kPa. The hypersonic stagnation pressure transducer will provide estimates of density and dynamic pressure but will yield little to no information about the wind environment. It is anticipated that the algorithm developed in this paper can augment the single pressure measurement to provide estimates of winds along with a redundant estimate of density and dynamic pressure. The atmospheric states reconstructed from this algorithm can also be used to initialize the filter that processes the supersonic pressure measurements as the transducers de-saturate. Furthermore, the algorithm can serve as a backup in the event of supersonic transducer failures or anomalies.

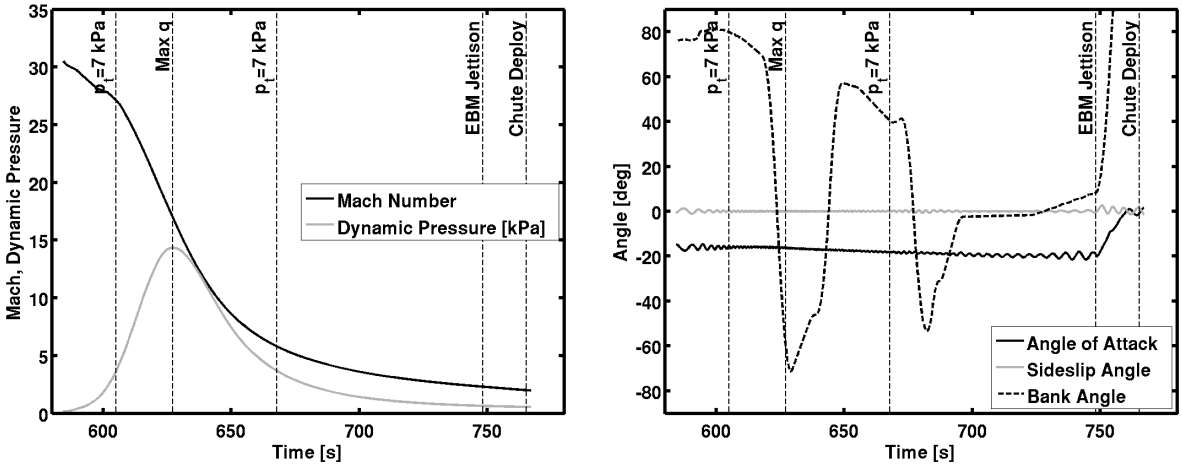

(a) Dynamic Pressure and Mach Number

(b) Flow Angles

Figure 11: Mars 2020 Reference Trajectory

The following figures show the results of a linear covariance analysis of the synthetic air data sensing algorithm applied to a representative Mars 2020 entry trajectory. The reference trajectory used for this analysis is shown in Fig. 11. Note that the supersonic FADS measurements are saturated over the time period from 605 s to 668 s. The synthetic air data method is compared against results of a single pressure port FADS air data estimate from the stagnation pressure port in the hypersonic flight regime, and a complete array of six pressure measurements in the supersonic regime. To stress the estimators, large a priori atmosphere uncertainties are used for this analysis, consisting of 15% uncertainty in density and pressure, 50 m/s in horizontal winds and 10 m/s in downward winds (all specified at the 3σ level). The IMU model is based on the MSL flight hardware as described in Ref. 24. The FADS pressure sensor are modeled with a non-repeatability uncertainty of 0.05% full scale pressure, and a noise floor of 30 Pa. Hysteresis uncertainties are included as a time-varying zero offset, modeled as random walk.

Results of the linear covariance analysis of the two methods are shown in Figure 12. These results compare reconstructions of density, pressure, dynamic pressure, and Mach number. These results show that the SADS solutions produce estimates of density and dynamic pressure with higher uncertainties than the FADS algorithm. The incorporation of the hydrostatic process model enables the SADS estimator to produce estimates of static pressure that are similar to that of the FADS state estimator, although slightly less precise. A similar trend appears in the Mach number estimate uncertainty.

A comparison of the wind estimate uncertainties is shown in Fig. 13. The SADS estimates provide some enhancement of the wind estimates during the hypersonic flight regime where the low scale supersonic pressure sensors are saturated. This effect is most noticeable in the north component, which is essentially a cross wind for this entry trajectory. The single hypersonic transducer provides estimates similar to the SADS method for the east (headwind) component. The FADS estimates are superior in all components in supersonic flight regime, where all pressure measurements are utilized.

Similar trends are evident in the aerodynamic flow angle uncertainties, shown in Fig. 14. The SADS approach can improve on the FADS results during the period where the supersonic pressure transducers are saturated. The FADS method using all pressure transducers is far superior in the supersonic flight regime, where the aerodatabase uncertainties are highest.

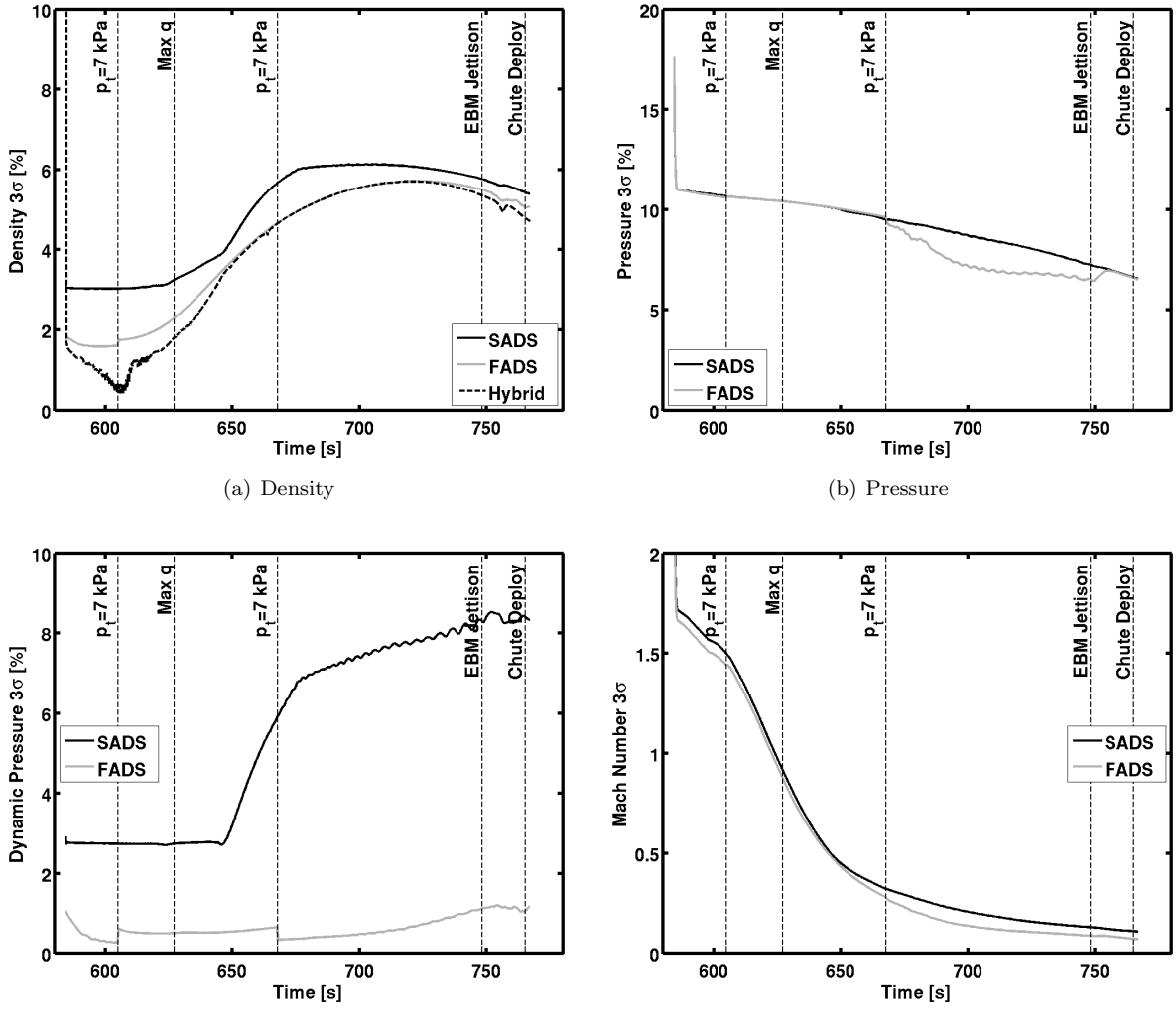

(a) Density

(b) Pressure

(c) Dynamic Pressure

(d) Mach Number

Figure 12: Comparison Between SADS and FADS - Density, Pressure, Dynamic Pressure, and Mach Number Uncertainties

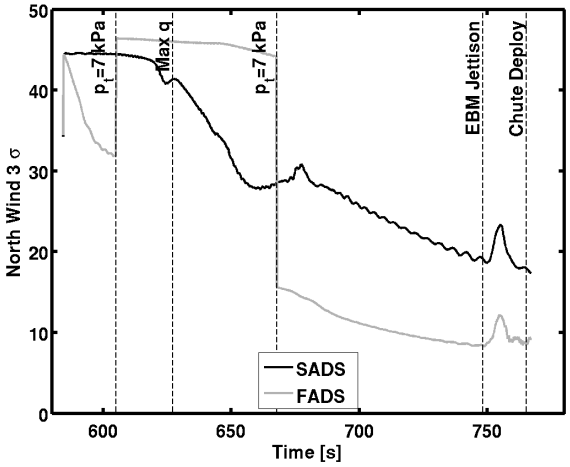

(a) North Wind

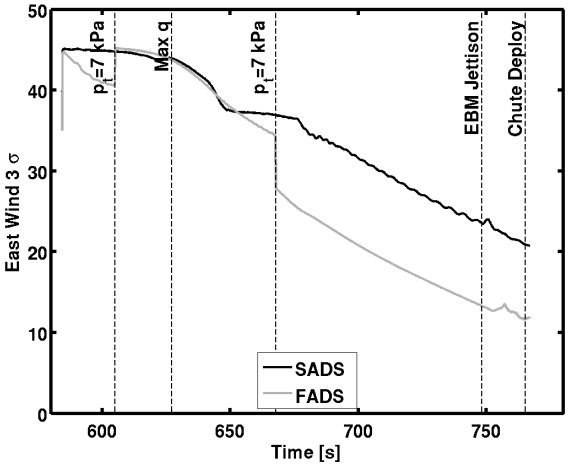

(b) East Wind

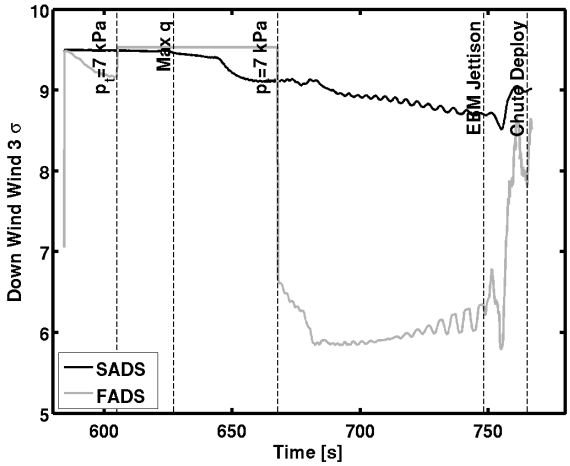

(c) Down Wind

Figure 13: Comparison Between SADS and FADS - Wind Uncertainties

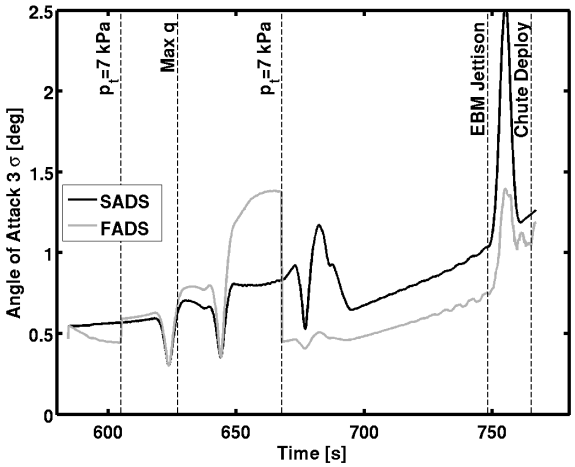

(a) Angle of Attack

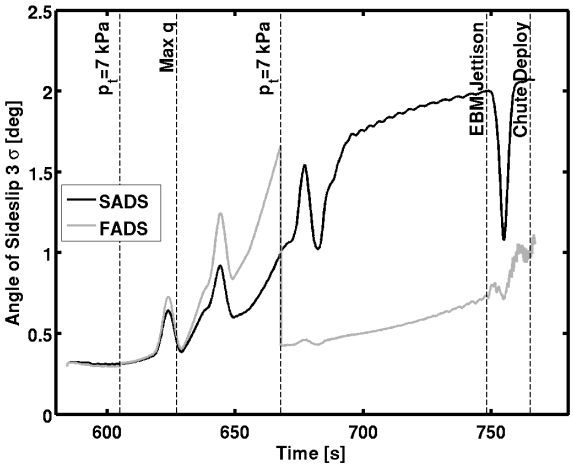

(b) Angle of Sideslip

Figure 14: Comparison Between SADS and FADS - Flow Angle Uncertainties

V. Conclusions

An estimator suitable for planetary probe entry atmosphere estimation has been developed. This estimator is based on the assumed nominal aerodynamic database (forces and moments) combined with in-flight measurements of the vehicle aerodynamics computed from inertial measurement unit data (accelerations and rates). The atmospheric states (winds, density, and pressure) are estimated using a nonlinear Kalman-Schmidt filter approach in which the inertial state of the vehicle (position, velocity, and attitude) are assumed to be known from the navigation system, and the atmosphere states are solved for from the measured aerodynamic forces and moments. A test case with flight data from the Mars Science Laboratory mission shows that the method performs well and is consistent with atmosphere states independently estimates from a flush air data system.

The method is expected to be utilized to aid the Mars 2020 entry air data system by providing additional data during periods in which the low pressure range transducers are saturated (above 7 kPa). Linear covariance analysis indicates that the synthetic method produces air data estimates with higher uncertainties than a true flush air data sensing system. Although the uncertainties in the derived atmosphere using the assumed aerodynamic model are higher than those computed from a traditional flush air data system, the proposed method provides a low cost alternative for atmosphere estimation. The method can be implemented in real-time and has the potential to be used in the on-board guidance and control. This approach could be used as in this manner as a primary air data system, or as a secondary/backup system for a traditional flush air data system.

References

[1]Adler, M., Wright, M., Campbell, C., Clark, I., Engelund, W., and Rivellini, T., "Entry, Descent, and Landing Roadmap: Technology Area 09," NASA, April 2012.

[2]Pruett, C. D., Wolf, H., Heck, M. L., and Siemers, P. M., "Innovative Air Data System for the Space Shuttle Orbiter," *Journal of Spacecraft and Rockets*, Vol. 20, No. 1, 1983, pp. 61–69.

[3]Nebula, F., Palumbo, R., Morani, G., and Corraro, F., "Virtual Air Data System Architecture for Space Reentry Applications," *Journal of Spacecraft and Rockets*, Vol. 46, No. 4, 2009, pp. 818–828.

[4]Seiff, A., "Possibilities for Determining the Characteristics of the Atmospheres of Mars and Venus from Gas-Dynamic Behavior of a Probe Vehicle," NASA TN D-1770, 1963.

[5]Nier, A. P., Hanson, W. B., McElroy, M. B., Seiff, A., and Spencer, N. W., "Entry Science Experiments for Viking 1975," *Icarus*, Vol. 16, 1972, pp. 74–91.

[6]Seiff, A., Reese, D. E., Sommer, S. C., Kirk, D. B., Whiting, E. E., and Neimann, H. B., "PAET, An Entry Probe Experiment in the Earth's Atmosphere," *Icarus*, Vol. 18, 1973, pp. 525–563.

[7]Seiff, A., "The Viking Atmospheric Structure Experiment - Techniques, Instruments, and Expected Accuracies," *Space Science Instrumentation*, Vol. 2, 1976, pp. 381–423.

[8]Kutty, P., "Reconstruction and Uncertainty Quantification of Entry, Descent and Landing Trajectories Using Vehicle Aerodynamics," M. S. Thesis, School of Aerospace Engineering, Georgia Institute of Technology, May 2014.

[9]Kutty, P. and Karlgaard, C. D., "Mars Science Laboratory Aerodatabase Trajectory Reconstruction and Uncertainty Assessment," AIAA Paper 2014-1094, January 2014.

[10]Kelly, G. M., Findlay, J. T., and Compton, H. R., "Shuttle Subsonic Horizontal Wind Estimation," *Journal of Spacecraft and Rockets,* Vol. 20, No. 4, 1983, pp. 390–397.

[11]Kutty, P. and Karlgaard, C. D., "Mars Science Laboratory Entry, Descent, and Landing Trajecotory Reconstruction Uncertainty Assessment," 10th Interplanetary Probe Workshop, San Jose, CA, June 2013.

[12]Koifman, M. and Bar-Itzhack, I. Y., "Inertial Navigation System Aided by Aircraft Dynamics," *IEEE Transactions on Control Systems Technology*, Vol. 7, No. 4, 1999, pp. 487–493.

[13]Lie, F. and Gebre-Egziabher, D., "Synthetic Air Data System," *Journal of Aircraft*, Vol. 50, No. 4, 2013, pp. 1234–1249.

[14]Velasco-Carrau, J., Garcia-Nieto, S., Salcedo, J. V., and Bishop, R. H., "Multi-Objective Optimization for Wind Estimation and Aircraft Model Identification," *Journal of Guidance, Control, and Dynamics*, to be published.

[15]Crassidis, J. L. and Junkins, J. L., *Optimal Estimation of Dynamic Systems, Second Edition*, Chapman & Hall, Boca Raton, FL, 2011.

[16]van Loan, C. F., "Computing Integrals Involving the Matrix Exponential," *IEEE Transactions on Automatic Control*, Vol. AC-23, No. 3, 1978, pp. 396–404.

[17]Rauch, H. E., Tung, F., and Striebel, C. T., "Maximum Likelihood Estimates of Linear Dynamic Systems," *AIAA Journal*, Vol. 3, No. 8, 1965, pp. 1445–1450.

[18]Ektin, B., *Dynamics of Atmospheric Flight*, John Wiley and Sons, Inc., New York, 1972.

[19]Steltzner, A. D., San Martin, A. M., Rivellini, T. P., Chen, A., and Kipp, D., "Mars Science Laboratory Entry, Descent, and Landing System Development Challenges," *Journal of Spacecraft and Rockets*, Vol. 51, No. 4, 2014, pp. 994–1003.

[20]Munk, M. M., Little, A., Kuhl, C., Bose, D., and Santos, J., "The Mars Science Laboratory (MSL) Entry, Descent, and Landing Instrumentation (MEDLI) Hardware," AAS Paper 13-310, February 2013.

[21]Karlgaard, C. D., Beck, R. E., O'Keefe, S. A., Siemers, P. M., White, B. A., Engelund, W. C., and Munk, M. M., "Mars Entry Atmospheric Data System Modeling and Algorithm Development," AIAA Paper 2009-3916, June 2009.

[22]Cheatwood, F. M., Bose, D., Karlgaard, C., Kuhl, C. A., Santos, J. A., and Wright, M. J., "Mars Science Laboratory (MSL) Entry, Descent, and Landing Instrumentation (MEDLI): Complete Flight Data Set," NASA TM-2014-218533, October 2014.

[23]Karlgaard, C. D., Van Norman, J., Siemers, P., Schoenenberger, M., and Munk, M., "Mars Entry Atmospheric Data System Modeling, Calibration, and Error Analysis," NASA TM-2014-218535, October 2014.

[24]Karlgaard, C. D., Kutty, P., Schoenenberger, M., Munk, M. M., Little, A., Kuhl, C. A., and Shidner, J., "Mars Science Laboratory Entry Atmospheric Data System Trajectory and Atmosphere Reconstruction," *Journal of Spacecraft and Rockets*, Vol. 51, No. 4, 2014, pp. 1029–1047.

[25]Chen, A., Cianciolo, A., Vasavada, A., Karlgaard, C., Barnes, J., Cantor, B., Hinson, D., Kass, D., Lewis, S., Mischna, M., Rafkin, S., Tyler, D., "Reconstruction of Atmospheric Properties from the Mars Science Laboratory Entry, Descent, and Landing," *Journal of Spacecraft and Rockets*, Vol. 51, No. 4, 2014, pp. 1062–1075.

[26]Schoenenberger, M., Van Norman, J., Karlgaard, C. D., Kutty, P., and Way, D., "Assessment of the Reconstructed Aerodynamics of the Mars Science Laboratory Entry Vehicle," *Journal of Spacecraft and Rockets*, Vol. 51, No. 4, 2014, pp. 1076–1093.

[27]Bose, D., White, T., Mahzari, M., and Edquist, K., "Reconstruction of Aerothermal Environment and Heatshield Response of Mars Science Laboratory," *Journal of Spacecraft and Rockets*, Vol. 51, No. 4, 2014, pp. 1174–1184.

[28]Holstein-Rathlou, C., Maue, A., and Withers, P., "Atmospheric Studies from the Mars Science Laboratory Entry, Descent and Landing Atmospheric Structure Reconstruction," *Planetary and Space Science*, Vol. 120, No. 1, 2016, pp. 15-23.

[29]Karlgaard, C. D., Kutty, P., and Schoenenberger, M., "Coupled Inertial Navigation and Flush Air Data Sensing Algorithm for Atmosphere Estimation," *Journal of Spacecraft and Rockets*, to appear.

[30]Tyler, D., Barnes, J., and Skyllingstad, E., "Mesoscale and Large-Eddy Simulation Model Studies of the Martian Atmosphere in Support of Phoenix," *Journal of Geophysical Research*, Vol. 113, No. E3, 2008.

[31]Rafkin, S.C.R., Haberle, R., and Michaels, T., "The Mars Regional Atmospheric Modeling System (MRAMS): Model Description and Selected Simulations," *Icarus*, Vol. 151, pp. 228-256.

[32]Vasavada, A. R., Chen, A., Barnes, J. R., Burkhart, P. D., Cantor, B. A., Dwyer-Cianciolo, A. M., Fergason, R. L., Hinson, D. P., Justh, H. L., Kass, D. M., Lewis, S. R., Mischna, M. A., Murphy, J. R., Rafkin, S. C. R., Tyler, D., and Withers, P. G., "Assessment of Environments for Mars Science Laboratory Entry, Descent, and Surface Operations," *Space Science Reviews*, Vol. 170, 2012, pp. 793–835.

[33]Serricchio, F., San Martin, A. M., and Wong, E. C., "The MSL Navigation Filter," 10th Interplanetary Probe Workshop, San Jose, CA, June 2013.

[34]Mendeck, G. and McGrew, L., "Entry Guidance Design and Postflight Performance for 2011 Mars Science Laboratory Mission," *Journal of Spacecraft and Rockets*, Vol. 51, No. 4, 2014, pp. 1094–1105.

[35]Way, D., Davis, J., and Shidner, J., "Assessment of the Mars Science Laboratory Entry, Descent, and Landing Simulation," AAS Paper 13-420, February 2013.

[36]Schoenenberger, M., Dyakonov, A., Buning, P., Scallion, W., and Van Norman, J., "Aerodynamic Challenges for the Mars Science Laboratory Entry, Descent, and Landing," AIAA Paper 2009-3914, June 2009.

[37]Dyakononv, A., Schoenenberger, M., and Van Norman, J., "Hypersonic and Supersonic Static Aerodynamics Mars Science Laboratory Entry Vehicle," AIAA Paper 2012-2999, June 2012.

[38]Hwang, H., Bose, D., White, T., Wright, H., Schoenenberger, M., Kuhl, C., Trombetta, D., Santos, J., Oishi, T., Karlgaard, C., Mahzari, M., and Pennington, S., "Mars 2020 Entry, Descent and Landing Instrumentation 2 (MEDLI2)," AIAA Paper 2016-3536, AIAA Thermophysics Conference, June 1016.